ELSEVIER

Effect of speed and accuracy of on-line elemental analysis on flotation control performance

A. Remes [a,*], K. Saloheimo [b], S.-L. Jämsä-Jounela [a]

[a] Department of Chemical Engineering, Helsinki University of Technology, P.O. Box 6100, 02015 HUT, Finland
[b] Outokumpu Technology, P.O. Box 84, 02201 Espoo, Finland

Abstract

In this paper the control performance of the flotation process is evaluated as a function of the measurement accuracy and sampling frequency of an on-stream analyzer. First, the performance of rule-based control and model predictive control (MPC) strategies is studied using discrete flotation models and the respective performance indices. Next, the net smelter return (NSR) is calculated for varying sampling rate and accuracy combinations using the PI controllers-based control strategy, mechanistic flotation models and the industrial process data as input. The control and economical performance of the process declines strongly when the sampling cycle is increased. The results also indicate that the speed of on-line analysis has a significant effect on the production economics, calculated as the average net smelter return.

© 2007 Elsevier Ltd. All rights reserved.

Keywords: Flotation; On-stream analysis; Economical optimization; Control performance; Sampling frequency; Measurement accuracy; MPC

1. Introduction

Flotation control, either operator-based or automatic, is dependent on the primary information provided by the plant instrumentation, on-stream analyzers and laboratory. Obviously, the accuracy of the measurements is translated directly into the accuracy of the controlled variables in the process. Together with the variation in ore feed and the dynamic behaviour of the multiple process stages and single unit processes, the time-dependent nature of the measurements (measurement delay and sampling frequency) is also a significant factor affecting the performance of process control.

In current base metal flotation processes a common practice is to use X-ray fluorescence (XRF) analyzers for the on-line measurement of metal concentrations in the principal slurry streams in the circuits. The analytical accu-

racy and sampling frequency of the concentration measurements both have an influence on the precision with which the process control can keep the process in optimal conditions. With a long cycle time, however, the state of the process may change before a new measurement becomes available. On the other hand, with shorter measurement times the statistical error of the analysis increases, resulting in less accurate control. The total error in measurement accuracy and sampling frequency can be minimized by optimizing the combination of measurement time and cycle time for each of the slurry lines analyzed.

A number of studies have dealt with the importance of accuracy and precision of on-line analysis for flotation control. Cooper (1976) investigated the measurement accuracies of the in-stream and multiplexed on-stream approaches, and estimated the return on the analyzer investment. The relationship between on-stream analysis accuracy and controlled concentrate grade–recovery was studied by Flintoff (1992). Tenno and Jämsä-Jounela (1996) studied the use of Monte Carlo simulation in evaluating the investment in a new control system or analyzer,

* Corresponding author.
  E-mail addresses: antti.remes@tkk.fi (A. Remes), sirkka-l@hut.fi (S.-L. Jämsä-Jounela).

and concluded that selection of the flotation operating point and accuracy of the analyzer strongly affect the resulting profit.

In this paper, the control performance of the rule-based control and model predictive control (MPC) strategies is first studied using the discrete flotation models and the respective performance indices. Discrete step response models have been reproduced from the models developed by Hodouin et al. (2000). Next, an evaluation of the economical performance of the flotation circuit at the Inmet Mining Co. Pyhäsalmi mine is carried out based on the use of the mechanistic flotation models. Several different, well-established dynamic flotation models have been presented in the literature. Niemi (1966) applied first-order linear differential equations based on kinetic flotation rate coefficients. These rate coefficients were determined in an industrial plant by performing tracer experiments. Bascur (1982) presented a detailed phenomenological model of flotation, based on the population balances and transfer of particles between the different phases in a cell. The phases for mineral particles in the flotation were defined as: free in the pulp, attached to the pulp, free in the froth and attached to the froth. Thus, the model depicts the behaviour of the different mineralogical species and sizes in each of the phases. In addition, Moys (1984) developed a model for the movement in two dimensions of the froth stream towards the concentrate weir. The model was formulated in terms of the cell design and the control variables and froth stability. In this paper the superimposed flotation and control model is used for a non-steady-state study of the flotation performance based on the net smelter return in terms of the configuration parameters of on-line elemental analysis. The model is based on first-order flotation kinetics as presented in Niemi (1966). Estimation of a small number of parameters is required for the model to be used together with industrial data. The use of this type of model

for studying the flotation performance problem was motivated by the excellent results reported by Bazin and Hodouin (2000).

2. Speed and accuracy of the on-line elemental analysis

For successful control of the flotation process, the XRF analyzer has to be carefully designed and calibrated for the process in question. The analysis speed of an XRF analyzer is strongly dependent on how the measurement is configured. One of the analysis error components is due to the random variance of the counted intensities. This component is inversely proportional to the measurement time, i.e. the relative variance decreases when the number of counted pulses becomes larger. As a general rule, the more X-rays available in the primary radiation and can be counted by the detector system, the faster the measurement can be performed in order to achieve the satisfactory accuracy. The measurement error due to the XRF pulse intensities can be calculated as

$$\sigma_{\text{pulse}} = \frac{\sqrt{(I_{\text{tot}} + I_{\text{background}}) \cdot 60 \cdot T}}{I_{\text{tot}} \cdot 60 \cdot T}, \tag{1}$$

where I_{tot} (1/s) and $I_{\text{background}}$ (1/s) are the total and background intensities of the detected X-ray fluorescence, and T (min) is the measurement time.

The accuracy of the analysis is also dependent on how the slurry sample is taken and how it is presented for analysis. Owing to X-ray absorption by water and solids, the measured fluorescence occurs in a thin (less than 1 mm for most elements of interest) layer immediately in front of the plastic window separating the continuously flowing sample from the X-ray source and detector, as shown in Fig. 1. Slurry flow in the measurement cell is of fundamental importance for the overall accuracy. The cell design must ensure that all particle sizes are equally represented
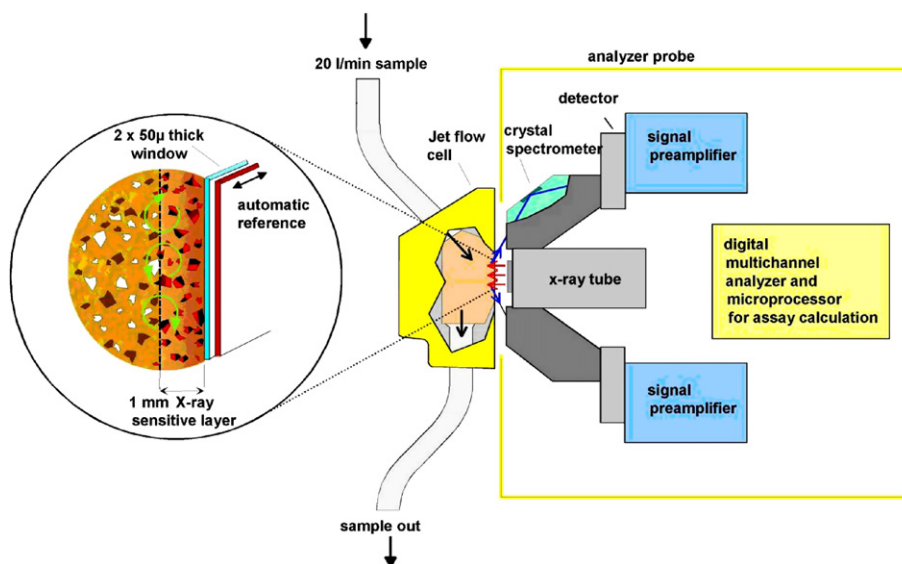

Fig. 1. XRF analyzer flow cell and analysis technology.

at the surface of the window. The window must remain clean and the sample in the sensitive volume must be representative and free from air. In addition, the accuracy of XRF analysis is affected by variation in particle size, sample composition, mineralogy and slurry density. Depending on the application, the relative analysis accuracy can vary between 1% and 10%.

The benefit of an analysis system depends on the resulting effects on the annual production value and on the annual operating costs of the analyzer. Cooper (1976) presented a formula for estimating the economical benefits of an XRF analyzer:

Annual value
$$= [\text{annual effects of the analyzer on the production} \\ \text{value } (ABC)] - [\text{annual costs of the analyzer}], \quad (2)$$

where the annual effects of the analysis system on the production value are divided into the components (*A*) availability, (*B*) functionality and (*C*) accuracy. The availability (*A*) describes the proportion of time out of the total plant operating time when the analysis system is also operating. Factor (*A*) can be further divided into the components A_1, describing the analyzer availability, and A_2 describing the sampling system availability. The sampling system availability is calculated using

$$A_2 = \frac{1}{1+S}, \quad (3)$$

where *S* is the number of daily operating breakages lasting over 10 min. The functionality (*B*) presents the analyzer measurements time in proportion to the process time constant. The last coefficient describing the analyzer accuracy (*C*), is obtained using

$$C = \frac{1}{1 + N\left[\dfrac{\sum S_C}{\sum S_P}\right]}, \quad (4)$$

where *N* is the number of analyzer measurements in the flotation circuit, S_C the analyzer measurement deviation and S_P the process deviation.

3. Effect of the analysis cycle time on flotation control performance

3.1. Discrete step response models of a rougher flotation bank

The effect of the assay cycle on flotation control performance is first studied with model predictive and rule-based control strategies. These are applied to the model of a rougher flotation bank presented by Hodouin et al. (2000). In addition to the model predictive control, a study on rule-based control is also included. This is a commonly used control strategy for flotation processes in practice. Fig. 2 shows a schematic diagram of the applied control
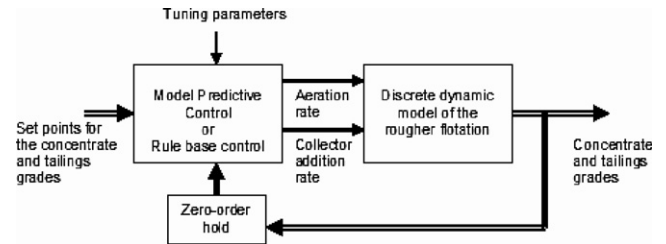

Fig. 2. Schematic diagram of the control strategies for the rougher flotation.

strategies. The analysis cycle is taken into account with the zero-order hold.

The discrete models are based on dynamic population balance models. The simulation model consists of two inputs: aeration rate (m³/min) and collector addition rate (g/min), two outputs: concentrate and tailings grades (%), and two disturbances: feed flow rate (ton/s) and feed grade (%). The discrete model equations are summarized in Table 1. Step response experiments, reproduced according to Hodouin et al. (2000), are shown in Fig. 3.

3.2. Applied control strategies

The effect of the assay cycle, and thus the control interval, was studied with the two different control strategies: model predictive control and rule-based control. The aim of the MPC is to keep the concentrate and tailings grades within the given set point values in the pre-defined, economically optimal operating point of the process. The generalized model predictive control consists of two manipulated inputs and two outputs. The MPC controller uses the plant models (Table 1) describing the dynamics of

Table 1
Transfer function models of the flotation process (according to Hodouin et al. (2000))

Concentrate grade	Tailings grade
$G_{c,air}(z) = \dfrac{-0.096z}{z^2 - 0.834z}$	$G_{t,air}(z) = \dfrac{-0.00092z^4 - 0.0008z^3}{z^5 - 1.62z^4 + 0.66z^3}$
$G_{c,collector}(z) = \dfrac{0.12z^4 - 0.16z^3}{z^5 - 1.66z^4 + 0.69z^3}$	$G_{t,collector}(z) = \dfrac{-0.0016z^4 - 0.0014z^3}{z^{14} - 1.59z^{13} + 0.63z^{12}}$
$G_{c,feedrate}(z) = \dfrac{1.68z^4 - 1.44z^3}{z^5 - 1.62z^4 + 0.65z^3}$	$G_{t,feedrate}(z) = \dfrac{0.0143z^4 + 0.01194z^3}{z^{11} - 1.53z^{10} + 0.59z^9}$
$G_{c,feedgrade}(z) = \dfrac{0.56z}{z^2 - 0.89z}$	$G_{t,feedgrade}(z) = \dfrac{0.0053z^4 + 0.0046z^3}{z^{14} - 1.6z^{13} + 0.64z^{12}}$

Reference values:
Metal content in the rougher concentrate: 15.7%.
Metal content in the rougher tailings: 0.19%.
Metal content in the rougher feed: 3.4%.
Feed rate: 0.2 ton/s.
Aeration rate: 13 m³/min.
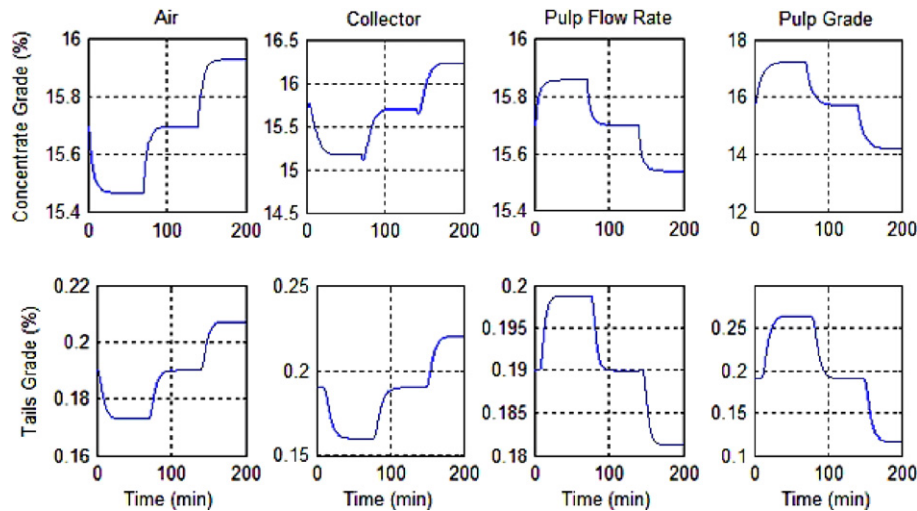Collector addition rate: 75 g/min.

Fig. 3. Responses of the concentrate and tailings grades to step changes in the aeration rate, collector addition rate, feed rate and feed grade.

the concentrate and tailings grades in relation to the aeration rate and collector addition. The controller computes the control actions that minimize the cost function *J* along the control interval

$$J(k) = \sum_{i=1}^{ne} \gamma_y [y_r(k+i) - \hat{y}(k+i)]^2 + \sum_{j=1}^{nu} \gamma_u \Delta u(k+j-1)^2.$$

(5)

With the notations: *k* – current discrete time; y_r – reference signal; $\hat{y}$ – predicted output signal; Δu – control signal increments; *ne* – prediction horizon; *nu* – control horizon; γ_y – output weighting factors for the control error; γ_u – weighting factors of the control increments.

Because of the non-linear behaviour of the flotation process, the discrete transfer functions used in the MPC are valid only around the reference values of Table 1. The output weights γ_y of the MPC cost function were set to 1 and 10 for the concentrate and tailings, respectively, and the input weights γ_u to the value of 0.1. The prediction horizon *ne* was set to 60 min and the control horizon *nu* was two times the control interval, which was varied from 6 to 30 min.

The control objective of the rule-based control is to keep the concentrate and tailings grades within the reference values. The rule-based control adjusts the collector addition rate on the basis of the concentrate grade, and the aeration rate on the basis of the tailings grades by applying small increments to the control variables. An optimization strategy that calculates the most economical flotation circuit set point is an issue that was not addressed in this study. Otherwise the control follows the commonly used rule-based control strategy in the concentrators.

3.3. Results of the control performance for different analysis cycles

The effect of the assay cycle on flotation performance was tested with both control strategies. The control results

were evaluated in terms of the integral square error (ISE), which describes the deviation of the measurement from the set point in terms of the sum of the squares. The following simulation schemes were applied: step changes in the concentrate (+1%, +1% and −1%) and tailings (+0.1%, +0.05% and −0.2%) without disturbances; disturbances (feed rate and grade) with the constant set points of the concentrate and tailings grades; and the set point changes in the concentrate and tailings grades when disturbances are present. The applied 'random walk' (Brownian motion) of the input disturbances is shown in Fig. 4.

The results of the control performance with the different assay cycles are presented in Table 2. The general trend is that a longer assay delay decreases the control performance, as indicated by the higher ISE indices. In most cases the model predictive controller gives better control performance than the rule-based control. However, it can be noted that in disturbance rejection – when no changes in the concentrate and tailings grade references are present
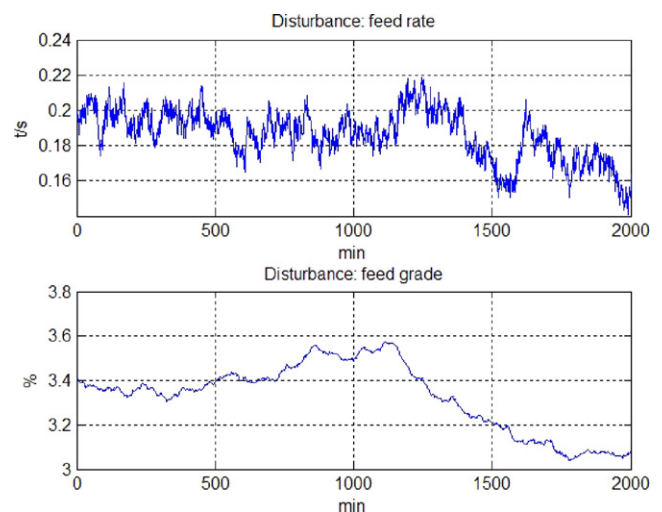

Fig. 4. Feed rate (ton/s) and grade (%) disturbances applied as an input sequence for the MPC and rule-based control of the rougher flotation.

Table 2
Values of the integral square error (ISE) for the model predictive control (MPC) and rule-based (RB) control with different control intervals, when the set point changes and disturbances are applied

Controller	Set point changes		Constant set point, input disturbances		Set point changes, input disturbances	
	Tailings	Concentrate	Tailings	Concentrate	Tailings	Concentrate
MPC_6	1.1	118.8	0.6	78.6	1.1	122.8
MPC_10	0.7	125.6	0.5	60.4	0.8	137.2
MPC_15	1.6	308.6	1.0	172.5	1.6	321.5
MPC_20	1.1	286.4	0.8	129.9	1.2	330.3
MPC_25	1.7	482.9	1.4	276.2	1.8	553.2
MPC_30	3.1	532.2	1.5	306.1	3.1	615.9
RB_6	11.1	247.3	0.1	25.6	10.9	372.7
RB_10	10.6	405.8	0.1	44.7	7.0	905.7
RB_15	12.2	650.3	0.1	73.9	6.2	1300.2
RB_20	13.0	813.1	0.1	166.3	7.0	1395.3
RB_25	13.8	913.0	0.4	334.0	7.0	1529.1
RB_30	14.8	1150.4	0.8	536.4	7.5	1712.2

– the rule-based control gives better ISE performance results with short (less than 15 min) control intervals. The controller performance can, however, be affected by tuning the weights when the applied assay cycle is selected, and the MPC can also operate better in this situation. Fig. 5 gives examples of the control results for the set point tracking and disturbance rejection for the MPC or rule-based control. The results give an indication of the importance of a sufficiently frequent assay cycle in flotation control. A more frequent cycle speeds up the control dynamics, and the concentrate and tailings grades can be kept more accurately within the set points.

4. Effect of the analysis cycle time and measurement time on the economical performance of the industrial flotation circuit

This study is focused on assessing the metallurgical performance of a flotation circuit as a function of the parameters of the on-stream analysis system. A model is required for both the dynamics of the flotation process and process control based on the on-stream assaying. Fig. 6 shows a schematic diagram of the system with the controller and the model which has been implemented in the PC-Matlab/Simulink environment.
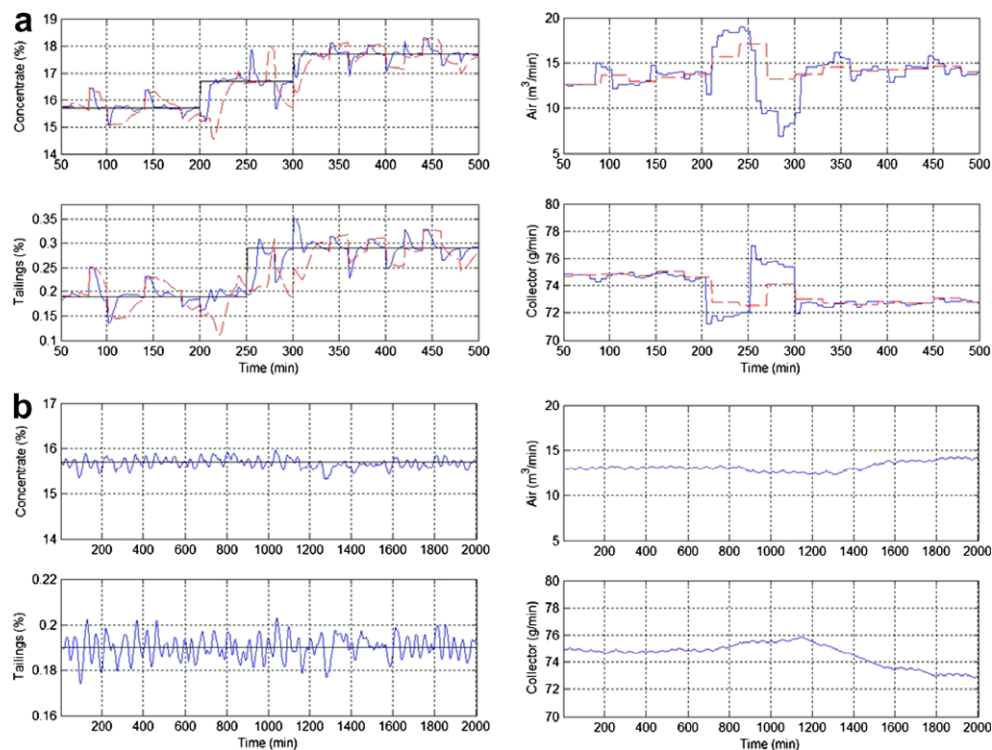

Fig. 5. Examples of the flotation control results showing the simulated concentrate and tailings grades and the manipulated aeration and collector addition rates with (a) model predictive control with 6 and 30 min control intervals and the set point changes in the concentrate and tailings grades and (b) rule-based control with a 6 min control interval and feed rate and grade disturbances.
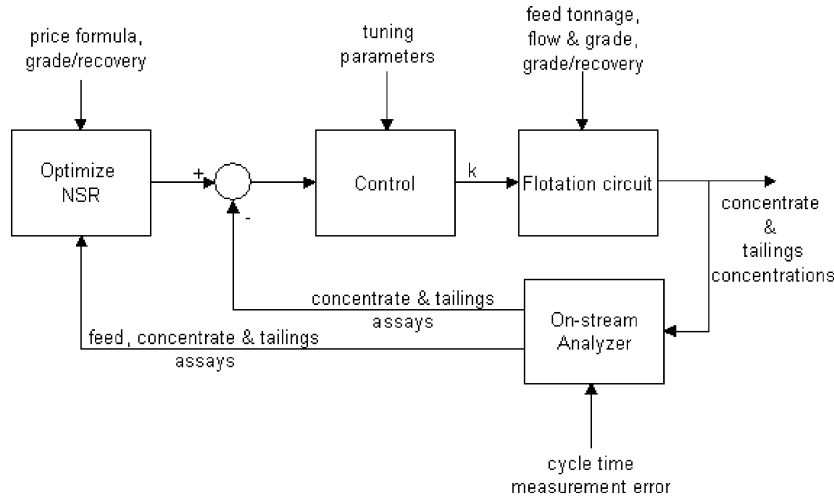
Fig. 6. Structure of the simulation system.

4.1. Modelling the flotation circuit

Flotation circuit modelling has been studied by various authors, and a number of models have been proposed. In this study, the main objective is to determine the behaviour of a flotation circuit under tight control. In order to model the metal concentrations in the main slurry streams, the classic first-order reaction kinetics equations are used to describe the flotation kinetics by means of a single parameter, the flotation kinetic rate coefficient. Simplifications are made, for example, by omitting the valve and pipe dynamics of the circuit in order to keep the number of experimental parameters reasonable.

Suppose that a slurry with flow F_f and metal concentration C_f based on the unit airless volume of the pulp is fed to a flotation stage with slurry volume V. It has been shown experimentally that the first-order kinetic equation applies to the flotation of sulphide minerals (Niemi, 1966 with further references). Assuming ideal mixing in the slurry (Jowett, 1972), and a uniform particle type in the flotation stage, the dynamic material balance can be written as

$$\frac{dm}{dt} = F_f C_f - F_t C_t - kVC_t, \tag{6}$$

from which the concentration of both the combined rougher/scavenger pulp and the tailings is obtained

$$\frac{dC_t}{dt} = \frac{1}{V}(F_f C_f - F_t C_t) - kC_t, \tag{7}$$

where F_f and F_t are the airless volumetric flow rates of the feed and tailings (dm³/min), C_t and C_f are the metal concentrations of the tailings and feed pulp (kg$_{metal}$/dm³) based on the unit airless volume, and k is the kinetic flotation rate coefficient (1/min). In Eqs. (6) and (7), the effect of the mass flow from the froth layer back into the pulp phase is also assumed to depend on the coefficient k and the pulp concentration C_t (Niemi, 1966). As a result, the coefficient k includes both the effects of the primary flotation and the return from the froth layer. The concentration of metals

passing from the pulp to the foam phase follows the first-order reaction equation, if the operation is under free flotation conditions. However, if the density of the slurry is high, the feed concentration is high, or the flotation air feed is low, then the process can be under inhibited flotation, where the area of the air bubbles is a limiting factor (Niemi, 1966; Jämsä-Jounela, 1990). Another condition that is not covered by Eq. (7) is when the structure of the foam limits efficient flow to the launder (Lynch et al., 1981). The kinetic flotation rate coefficient of the uncontrolled system can be obtained from Eq. (7) by assuming steady-state conditions

$$k = \frac{F_f C_f - F_t C_t}{V C_t} = \frac{F_c C_c}{V C_t}, \tag{8}$$

where F_c is the airless volumetric concentrate flow rate (dm³/min) and C_c is the concentration of the concentrate based on the unit airless pulp volume (kg/dm³).

In addition to the pure metal mass transfer into the concentrate flow according to Eq. (6), the volumetric flow rates need to be solved. Thereby, the water balance equations are defined. Here, the objective is to calculate the water recovery using measurements obtained with industrial flotation instrumentation. The water flow rate in the concentrate $F_{w,c}$ (dm³/min) is bound to the recovery value R (%) by the water retention coefficient k_w (dm³/min) (Lynch et al., 1981),

$$F_{w,c} = k_w R. \tag{9}$$

Assuming the ore density to be constant, the incoming water flow in the feed $F_{w,f}$ (dm³/min) is obtained using the total feed flow F_f, the ore mass flow $m_{ore,f}$ (kg/min) and the ore density ρ_{ore} (kg/dm³),

$$F_{w,f} = F_f - m_{ore,f}/\rho_{ore}. \tag{10}$$

Finally, the total volumetric concentrate flow is obtained by taking the froth washing and launder water into account. The last term in Eq. (6) represents the mass flow of pure metal to the concentrate. The dry solid mass flow

of the concentrate m_c (kg/min) is obtained from kVC_t by dividing by the mass percentage content of the produced concentrate c_c (%). Using the solid density of the concentrate $\rho_{c,solid}$ and the concentrate water flow $F_{w,c}$, the tailings flow rate F_t (dm^3/min) can be calculated

$$F_t = F_f - m_c/\rho_{c,solid} - F_{w,c}. \tag{11}$$

In Eq. (11), the volume of the cell remains approximately constant and, when the feed flow fluctuates, the fluctuation also appears immediately in the tailings flow. The dynamics of the valve and outflow pipe are also neglected. Instead, the mass flows are delayed due to the cell dynamics according to Eq. (6).

In a flotation plant, the separation dictating the recovery mainly occurs in the rougher and scavenging flotation banks, while the cleaning stage is responsible for the grade improvement. Equally, in the flotation circuit model the flotation kinetic equation (6) is applied together in these units. Thus, the pulp volume V can be reasonably approximated to be the sum of the cell unit volumes. Furthermore, the time delay between the feed and tailings is also dictated by the process delay. In contrast, the delay from the feed to the concentrate is modelled as a dead time, due to the cleaner cells. An approximation of the delay is determined using the cross-correlation analysis of the industrial model input data. Selection of this type of model approximation for the rougher/scavenging flotation was considered to be justified due to the fact that, in industrial sites, usually only a few on-line measurements of the concentration assays are available, as was the case in the industrial test site of this study.

4.2. Grade–recovery relationship

The concentrate grade is determined using a static grade–recovery model covering the whole flotation circuit. The recovery R (%) of the metal in the flotation circuit is calculated according to the following equation:

$$R\% = \frac{\dot{m}_{c,met}}{\dot{m}_f \cdot f} \cdot 100\%. \tag{12}$$

The circuit recovery R (%) is defined as the ratio of the final concentrated metal $\dot{m}_{c,met}$ (kg/min) to the metal fed into the
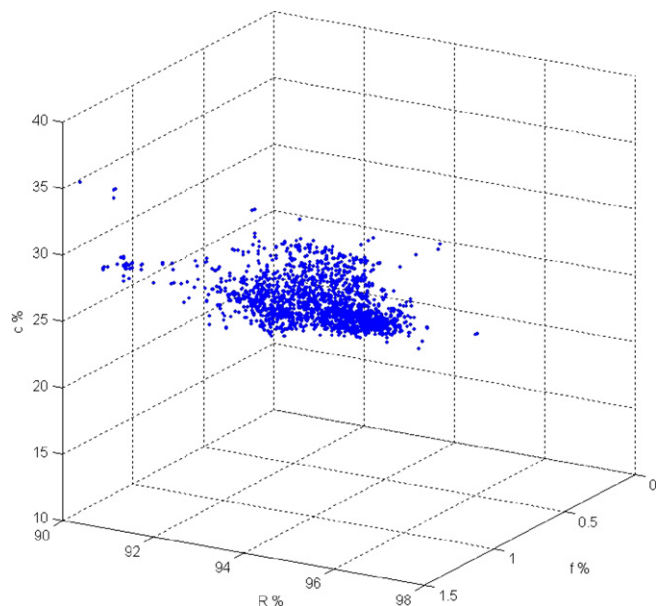

Fig. 7. Feed (f, %), concentrate (c, %) and recovery (R, %) data from an industrial flotation circuit.

circuit $\dot{m}_f \cdot f$ (kg/min), where f is the feed metal content. In Eq. (12) the metal content in the final concentrate $\dot{m}_{c,met}$ of the circuit is shifted backwards with a time delay that best correlates with the circuit dynamics between the feed and the final concentrate.

Estimation of the dependence of the grade recovery on the process data is not a straightforward task. Typical data points of the feed (%), concentrate (%) and recovery (%) values of an industrial copper flotation circuit are shown in Fig. 7.

As can be seen from Fig. 7, the data points rarely form a smooth surface from which mathematical formulation of the feed-grade–recovery dependence could be estimated. In this case the data are clearly clustered in two areas (see the histograms in Fig. 8). The feed (%) is skewed to the right, and the concentrate (%) forms a two-peak distribution. This is due to the operational target of the flotation circuit, i.e. to achieve an optimal grade–recovery point.

Several types of model, including the second-order surface, an average grid and neural networks, were evaluated
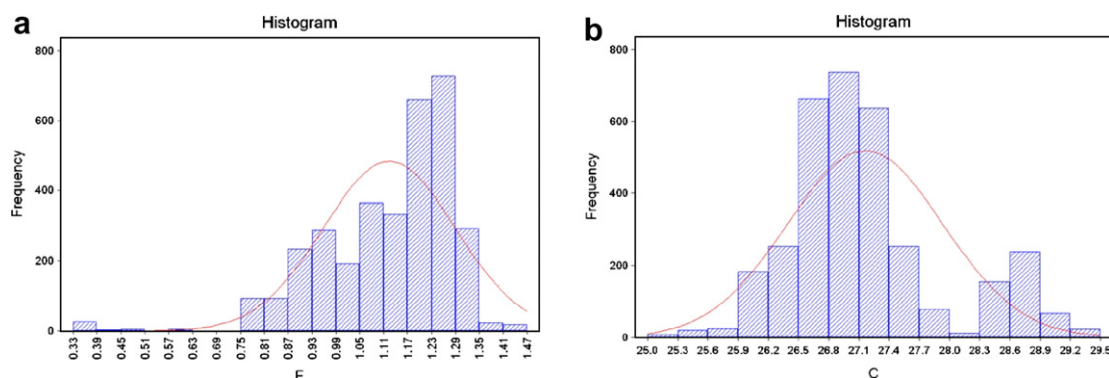

Fig. 8. (a) Feed and (b) concentrate flow grade (%) histograms from an industrial flotation circuit.

for fitting the data shown in Fig. 7. However, the best results were achieved with an exponential curve fitting. Eq. (13) was fitted to over 3000 data points using the least squares method,

$$R = R_{max}[1 - e^{((c-c_{max})/\alpha)}].\tag{13}$$

In Eq. (13), R (%) is the recovery, R_{max} (%) the maximum recovery, c (%) the concentration, c_{max} (%) the maximum concentration and α an estimated parameter. Eq. (13) was applied separately to the four data classes, in which the data points were classified into quartiles according to the feed (%) concentration. To avoid a spurious local minimum, the following constraints were applied: R should monotonously increase when c decreases, and R should monotonously increase when the feed (%) increases. The grade–recovery curves obtained are shown in Fig. 9.

In the dynamic flotation model, Eq. (3) determines the concentration of the rougher/scavenger tailing and cell pulp. The recovery is calculated from Eq. (13) and, finally, the concentration of the concentrate c (%) is obtained from Eq. (14) as follows:

$$c = \ln\left(1 - \frac{R}{R_{max}}\right)\alpha + c_{max}.\tag{14}$$

The notations are according to Eq. (13). Thus, Eq. (14) transforms the rougher/scavenger recovery to the final concentrate grade, when used with the history data-fitted parameters incorporating the effect of recovery losses in the cleaning stage.

4.3. On-stream analyzer and assays

The on-stream analyzer dynamics was modelled by a zero-order hold circuit with a time delay describing the length of the analysis cycle. Thus, the assay value remains constant until a new update is obtained after the cycle time t_{cycle} has passed.
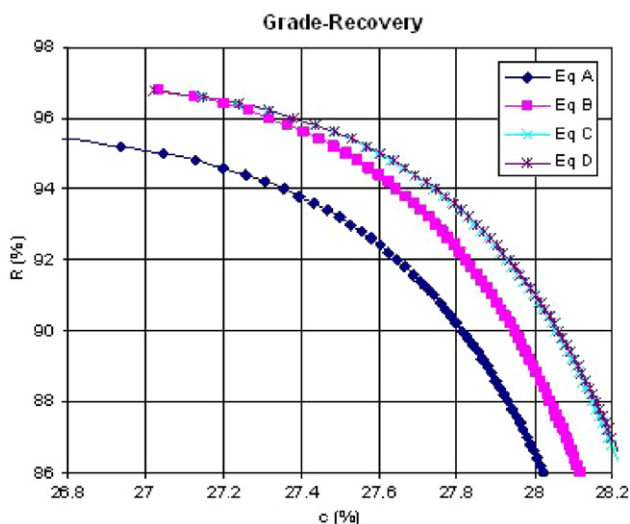

Fig. 9. Grade–recovery curves with different feed grades A, B, C and D, corresponding to the four feed quartiles of the sample data.
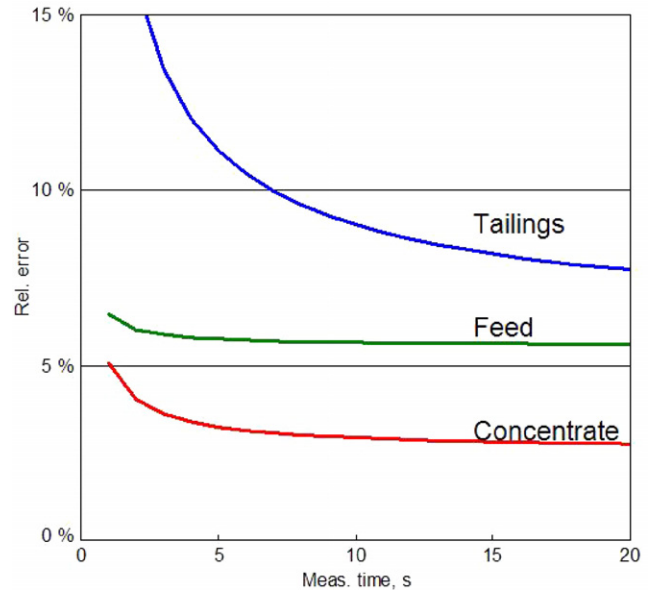

Fig. 10. Relative XRF assay errors as a function of the sample measurement time. The curves running downwards present the relative errors of the tailings, feed and concentrate assays.

The analysis accuracy was simulated by adding an additional random error to the 'actual' concentrations obtained from the model. In order to assess the effect of the sample measurement time, the random error was divided into two parts: a constant analysis error and a dynamic part accounting for the statistical component of the counted X-ray pulses p. The latter component is inversely proportional to the square root of the measurement time t_{meas},

$$\sigma_t = \sqrt{\sigma_{t0}^2 + (p^2/t_{meas})}, \quad jt_{cycle} < t < (j+1)t_{cycle},$$
$$j = 1, 2, 3, \ldots.\tag{15}$$

Thus, the simulated assays $\tilde{M}$ for a certain concentration C are

$$\widetilde{M}(t) = C(jt_{cycle} - \theta) + e_0(0, \sigma_0) + e_1(0, \sigma_1(t_{meas})),$$
$$jt_{cycle} < t < (j+1)t_{cycle}, \quad j = 1, 2, 3, \ldots,\tag{16}$$

where t_{cycle} is a cycle time, θ an assay delay, and $e(m, \sigma)$ a normally distributed random number with a mean m and a standard deviation σ. As the result of Eq. (15), Fig. 10 presents typical relative measurement errors as a function of the measurement time for the feed, concentrate and tailings assays. The calculations are based on the relative analysis errors of each measured line when 15 s measurement times were applied for analyzer calibration. The error dependence on the pulse counting time is obtained by applying Eq. (15). A practical minimum for the sample measurement time is around 10 s due to sample flow stabilization after a changeover. Thus, it can be deduced from these results that the increase in the measurement time does not significantly decrease the relative error in the feed and concentrate assays; instead the tailings assay error slightly decreases. However, the sampling frequency apparently

plays a more important role in the use of the assays for control purposes.

4.4. Control of the flotation circuit

In industrial flotation processes adjustment of the flotation rate, i.e. control of the process, is typically achieved by manipulating the chemical dosing, cell levels and the cell aeration (Hodouin et al., 2001; Kämpjärvi and Jämsä-Jounela, 2003). Studies on the dependence of the flotation rate coefficient *k* under certain conditions can be found in Niemi (1995) and Jämsä-Jounela (1990). Since the aim in this study is to study the dependence of the economical performance of flotation on the measurement quality, the control system itself is kept straightforward, assuming a well-performing control strategy. Thus, here the flotation performance is dependent only on the analysis system configuration providing assays with a certain quality and cycle. The control system in the model is based on a PI loop that adjusts the kinetic flotation rate coefficient *k* in Eq. (7). Here, the objective is to keep the final concentrate grade and/or tailing grade at the optimal set point, which is determined from the intersects of the grade–recovery curves and isoeconomic curves for each ore feed grade. The economic values, and subsequently the isoeconomic curves, are calculated from a formula for the net smelter return,

$$NSR = fR(C_1 - C_2 - C_3/c), \qquad (17)$$

where *f* is the feed concentration, *R* the recovery, C_1 the metal price, C_2 the treatment charge, C_3 presents the transport cost losses, and *c* is the concentration of the concentrate.

4.5. Process data of the Pyhäsalmi concentrator

The industrial case studied was the copper flotation circuit at the Inmet Mining Co. Pyhäsalmi Mine in Finland. The process flowsheet is shown in Fig. 11 and a more
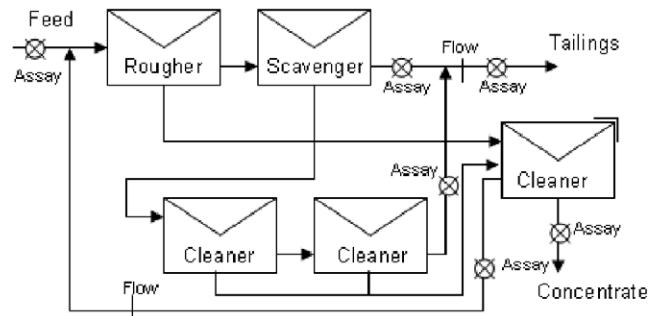

Fig. 11. Flowsheet of the copper flotation circuit at the Pyhäsalmi mine.

detailed description of the process and the on-stream analyzer system can be found in Lähteenmäki et al. (1999). The open flotation circuit, the well-maintained Courier® analyzer and advanced control strategy implemented in the Proscon® automation system, make this case ideal for our study.

The data used in the study consist of a 3-day sequence from February 2002. The assays were recorded once per minute, and the analyzer cycle was 5–6 min. Fig. 12 shows the data trends.

The residence time in the rougher/scavenger flotation cells was 24 min, as calculated from the feed volume flow rate and the flotation cell volume (8 Outokumpu OK-16 flotation machines). The first maximum in the cross-correlation between the feed and the concentrate assays occurs at a delay of 20 min. These cell volume and time delay values, as well as the ore properties and a grade–recovery relationship, were used in the model based on Eqs. (7)–(13), described earlier.

The fitted grade–recovery relationships at various feed grades are plotted in Fig. 13. These were used in the calculations to describe the average behaviour of the circuit. Several combinations of the measurement time and the analysis cycles were tested in the simulation runs, in order to cover the full range of reasonable values. Measurement
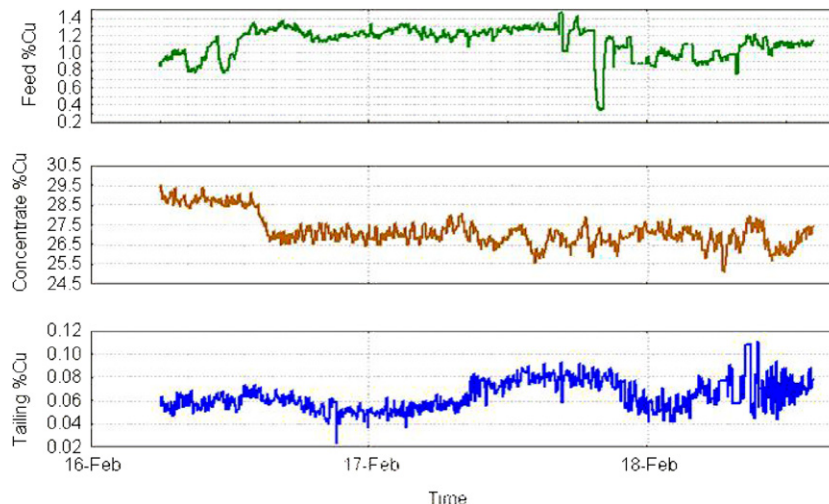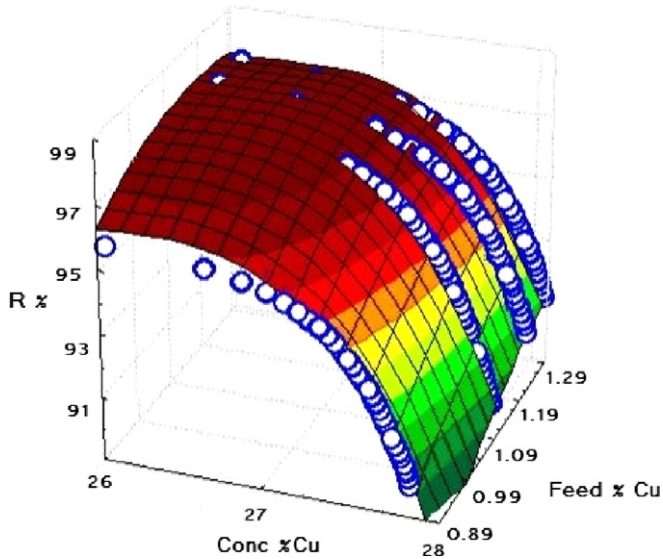

Fig. 12. The case assay data trends.

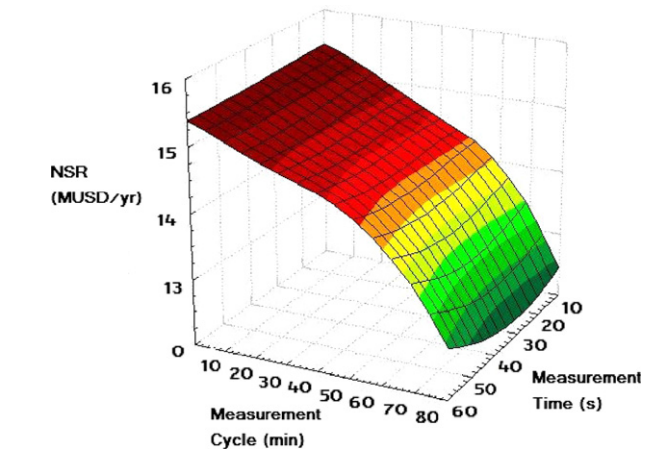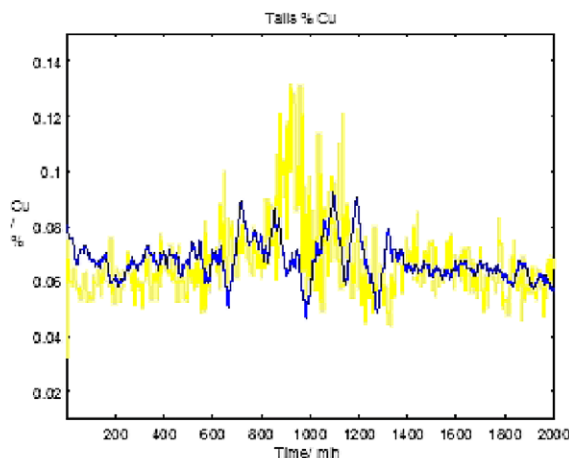Fig. 13. The grade–recovery model at various feed grades.

Fig. 15. The dependence of the net smelter return (scaled to one year of production) as a function of the analyzer cycle time and sample measurement time.

times smaller than 10 s were considered impractical since the analyzer system requires some time for the sample changeover and flow stabilization.

4.6. Simulation runs and model verification

The simulations were carried out on the basis of the feed grade assay, tonnage and flow rate history over the 3-day period. The optimal PI parameters for the controllers were determined at each cycle time. The concentrations were calculated for the net smelter return values, which were then rescaled to correspond to a yearly mining production value of 1.3 Mton. Fig. 14 shows the comparison plots of the simulated and the actual concentrate and tailings concentrations for an independent 33 h data set. The agreement for the model can be considered satisfactory. The simulated tailings grades follows the measurement values reasonably well. However, the behaviour of the concentrate can be seen to fluctuate more, most probably due to the limitations of the estimated grade–recovery relationship. The sig-

nal outliers were conditioned in the control system before using them.

4.7. Effect of the analysis cycle time and measurement time on flotation performance

The simulation runs were then performed for analysis of the effect of cycle time and measurement time on flotation performance. Fig. 15 shows the results of the simulation, as a function of the analyzer cycle time at various sample measurement times. The fluctuations are due to the random nature of the simulations, with the measurement error added as random numbers to the assay data. Fig. 16 shows a smoothed surface plot through the data.

It is evident from the results that the sample measurement time does not have a significant effect on the economical results. This can also be seen from Fig. 10; the measurement error does not change significantly when the measurement time is above 10 s.

The measurement cycle has a significant effect, at least in terms of the economical return. The difference between an
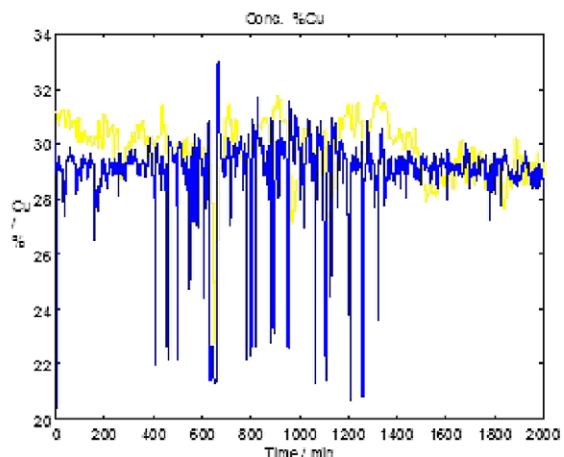

Fig. 14. Comparison between the simulated and measured feed and tailings assays.
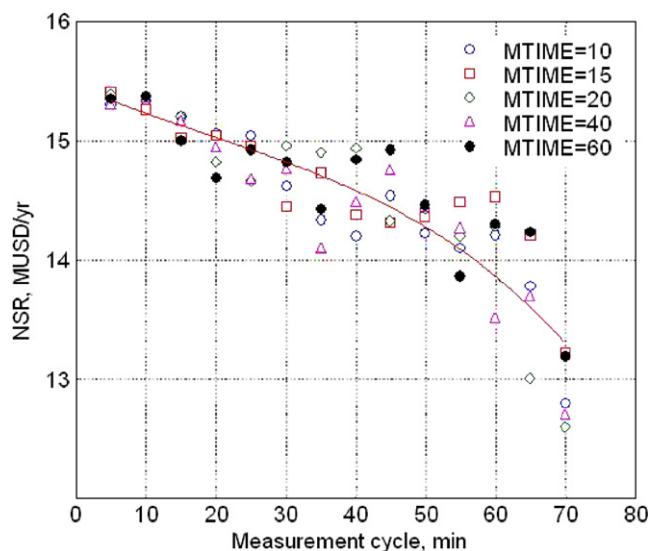
Fig. 16. A smoothed surface plot of the data shown in Fig. 13.

immediate measurement and a 40 min cycle is ca. 1 MUSD/year, which is lost in non-optimal control of the flotation circuit. The results are obtained by scaling the simulation results of the different periods to the annual production time (800 h) and mining production of 1.3 Mton/year. As an example, the difference in the simulated production value between the 40 and 5 min measurement cycles is ca. 6%. Also, fast sampling and analysis are recommended for control purposes, as far as the process time constant in this case is close to 20 min, and the sampling period is less than half of that. Nevertheless, the assays from the other process streams and the additional process measurements can be used to speed up the control dynamics. However, when the simulation results for the 5 and 15 min analysis cycles are compared, there is a difference of 100 kUSD/year (around 0.65%) in the production value.

In addition, the relative standard deviations of the assays for each slurry line (feed, concentrate and tailings) were studied as a function of the measurement cycle time. In practice, the analyzer measurement capacity is shared between several measurement lines. Therefore, there is a delay in the assays according to the number of lines. Typically, an analyzer system consists of six, 12 or even 24 multiplexed sample lines. Here, the simulations were carried out for the uncontrolled open loop process. The resulting optimal sample measurement times, which minimized the total assay deviations, were studied as a function of the measurement lines. In this specific case the optimal measurement times for the concentrate was 8 s and for the tailings 24 s, when six sample lines were used. Similarly, the optimal sample measurement times for a 12-line configuration were found to be 8 and 14 s, respectively. However, these results are only indicative, and give a general idea of the ratio of the required measurement times for each line. Nevertheless, the assay delay plays the most important role when the measurements are used for control purposes.

4.8. Applicability and limitations of the model

Obviously the implemented model needs to be refined through further research. Determination of a unique grade–recovery relationship may be problematic or, in some cases, even impossible. The grade–recovery dependence varies continuously due to changes in the ore type, as well as to variations in the particle size and in mineral liberation after the grinding stage. In addition, the lack of industrial measurements often constricts the grade–recovery relationship to cover the entire flotation circuit instead of individual cells.

In the applied model, the circuit recovery is assumed to be achieved primarily in the rougher/scavenger flotation. Thus, the tailings grades, and thereby the circuit recovery, is obtained using the first-order kinetic model applied to this part of the flotation. Subsequently, the cleaning phase of the flotation is considered as a time delay, which sets back the grades dictated by the data-fitted grade–recovery surface. Apparently, the intermediate process streams, especially the rougher concentrate and tailings assays, can be used to speed up the control dynamics in industrial applications. However, the main effects on flotation performance caused by analyzer speed and accuracy are clearly demonstrated by the studies using the kinetic flotation model and data-fitted parameter at the Pyhäsalmi concentrator copper circuit.

5. Conclusion and remarks

In this paper, the performance of the flotation process was studied as a function of measurement accuracy and sampling frequency. In the first case, the *rule-based control and model predictive control (MPC) strategies* were evaluated using the discrete step response models with the ISE index. The second simulation case was carried out using *the PI controllers-based control strategy*, *mechanistic flotation models* and industrial data as input. Evaluation was calculated with the net smelter return economical index. The results provide some quantitative information about the significance of analyzer accuracy and precision, as well as the speed of the analysis. The economical performance of the flotation circuit decreases drastically if the control actions are sufficiently delayed. This indicates the need for quick and accurate analysis to speed up the control dynamics. To reduce the error due to the measurement delay, fast basic measurements and control are necessary to complement the process analyzers, and to keep the process stable before the next assay arrives.

Acknowledgement

References

Bascur, O.A., 1982. Modelling and Computer Control of a Flotation Cell. University of Utah, Salt Lake City, 372 p.

Bazin, C., Hodouin, D., 2000. Tuning flotation circuit operation as a function of metal prices. CIM Bulletin 93, 93–99.

Cooper, H.R., 1976. On-Stream X-ray Analysis in Flotation. AIME, New York, p. 865.

Flintoff, B.C., 1992. Measurement issues in quality control. In: Proceedings of the 1992 Toronto CMP Branch Meeting, Toronto, pp. 2–6.

Hodouin, D., Bazin, C., Gagnon, E., Flament, F., 2000. Feedforward–feedback predictive control of a simulated flotation bank. Powder Technology 108, 173–179.

Hodouin, D., Jämsä-Jounela, S.-L., Carvalho, M.T., Bergh, L., 2001. State of the art and challenges in mineral processing control. Control Engineering Practice 9, 995–1005.

Jowett, A., 1972. Mathematical models of mineral processing operations in process control. The Chemical Engineer (268), 459–465.

Jämsä-Jounela, S.-L., 1990. Modern Approaches to Control of Mineral Processing. Acta Polytecnica Scandinavica. Mathematics and Computer Science Series, vol. 57, Helsinki, 33 p.

Kämpjärvi, P., Jämsä-Jounela, S.-L., 2003. Level control strategies for flotation cells. Minerals Engineering 16, 1061–1068.

Lynch, A.J., Johnson, N.W., Manlapig, E.V., Thorne, C.G., 1981. Developments in Mineral Processing. 3. Mineral and Coal Flotation Circuits, Their Simulation and Control. Elsevier, Amsterdam, 290 p.

Lähteenmäki, S., Miettunen, J., Saloheimo, K., 1999. 30 years of on-stream analysis at the Pyhäsalmi mine. Preprints of the 1999 SME Annual Meeting, Denver, pp. 1–6.

Moys, M.H., 1984. Residense time distribution and mass transport in the froth phase of the flotation process. International Journal of Mineral Processing 13, 117–142.

Niemi, A.J., 1966. A study of the dynamic and control properties of industrial flotation processes. Acta Polytechnica Scandinavica. Chemistry Including Metallurgy Series, vol. 48, Helsinki, 111 p.

Niemi, A.J., 1995. Role of kinetics in modelling and control of flotation plants. Powder Technology 82, 69–77.

Tenno, R., Jämsä-Jounela, S.-L., 1996. Copper flotation profit and control system accuracy. Control Engineering Practice 4 (11), 1545–1551.